Journal of the Korean Physical Society, Vol. 66, No. 7, April 2015, pp. 1144∼1148

Effect of Sulfur Incorporation on Solution-processed ZTO Thin-film Transistors

Sang-A Oh, Kyeong Min Yu, So-Hyun Jeong and Byung Seong Bae*
Department of Display Engineering, Hoseo University, Asan 336-795, Korea

Eui-Jung Yun
College of Green Energy Semiconductor Engineering and Department of System Control Engineering, Hoseo University, Asan 336-795, Korea

(Received 29 April 2014, in final form 12 February 2015)

In this research, we investigated the electrical properties of solution-processed sulfur (S)-incorporated zinc-tin-oxide (S-ZTO) thin-film transistors (TFTs). The best device characteristics, which include a threshold voltage of −0.74 V, a sub-threshold swing of 0.67 V/dec, an on/off current ratio of 8.31×10^5, and a mobility of 0.70 cm^2/Vs, were observed for 0.06-M S-ZTO TFTs. The device properties of the 0.06-M S-ZTO TFTs were similar to those of ZTO TFTs whereas the illumination stress stabilities and the hysteresis characteristics of the transfer curve for 0.06-M S-ZTO TFTs were better than those for ZTO TFTs. The X-ray diffraction analysis for the S-ZTO thin films also showed that tin (Sn) atoms bonded chemically with S atoms, suggesting that S atoms occupied oxygen sites, which, in turn, the reduced the number of oxygen vacancies. Therefore, the improved stabilities observed in S-ZTO TFTs are attributed to the reduction in the number of oxygen vacancies due to replacement of O by S.

PACS numbers: 81.05.Hd, 81.20.Fw
Keywords: Sol-gel, Solution process, Oxide TFT, Sulfur incorporated Zinc-Tin-Oxide TFT
DOI: 10.3938/jkps.66.1144

I. INTRODUCTION

For the backplane of a display such as a liquid crystal display (LCD) or an organic light-emitting display (OLED), hydrogenated amorphous silicon (a-Si:H) Thin-film transistors (TFTs), low-temperature poly-silicon (LTPS) TFTs, and oxide TFTs have been used [1–4]. The a-Si:H TFTs were used extensively for LCDs whereas LTPS TFTs were employed widely for OLEDs. Although a-Si:H TFTs allow a low-cost process for the display backplane, they are not suitable for high resolution, high frame rate and large area displays due to their low mobilities of less than 1 cm^2/Vs. The LTPS TFTs have the advantages of high mobility and good stability for high-resolution displays while their process costs are high due to the complex process. From these view points, the alternative device for the display backplane is an oxide TFT which has good transparency characteristics and a higher mobility than the a-Si:H TFT. However, oxide TFTs have stability issue, and much research regarding the stability issues has been reported [5–10].

Oxide TFTs have been extensively investigated for various applications, such as photo-detecting devices, biosensors, and flat-panel displays [11–19]. Also, many studies on solution-processed oxide TFTs have been reported due to their special advantages of using a simple printing process with a low cost [20]. The most representative channel layers used in solution-processed oxide TFTs are zinc-oxide (ZnO), indium-gallium-zinc-oxide (IGZO), and zinc-tin-oxide (ZTO) [21–23]. Solution-processed oxide TFTs are required to have outstanding electrical characteristics in order for them to be used in backplanes of displays. One way to achieve such excellent electrical characteristics is to dope metallic elements such as hafnium (Hf), lithium (Li), and titanium (Ti) into the oxide channel layers [24–26]. Doping with metallic elements improves the electrical properties. Recently, fluorine (F) doped ZnO TFTs were also reported to have high mobility and good stability for low-temperature process below temperatures 250 °C [27].

Chalcogen doping with elements such as S, selenium (Se) and tellurium (Te) have received attention [28,29], and the incorporation of S was reported to reduce the number of oxygen bonds [30]. Passivation with S has also been reported to remove oxides and produce a covalently-bonded S passivation layer on the indium-arsenide (InAs) and the germanium (Ge) [31, 32]. The replacement of

*E-mail: bsbae3@hoseo.edu; Fax: +82-41-540-5221

Table 1. Electrical parameters of ZTO TFTs at different sulfur concentrations.

Molar ratio	Vth (V)	S.S (V/decade)	I_{on}/I_{off}	Mobility (cm^2/Vs)
ZTO	1.08	0.62	6.56×10^5	1.15
0.30-M S-ZTO	9.07	1.20	3.49×10^4	0.12
0.24-M S-ZTO	9.84	0.85	1.02×10^4	0.12
0.18-M S-ZTO	9.17	1.21	1.25×10^4	0.20
0.12-M S-ZTO	8.03	0.59	7.87×10^4	0.13
0.06-M S-ZTO	−0.74	0.67	8.31×10^5	0.70

oxygen by S in the lattice was also observed for the S-incorporated ZnO [33]. Therefore, in this research, we investigated the effect of S incorporation on the electrical properties and the stability characteristics of the S-ZTO TFTs.

II. EXPERIMENTS

We fabricated oxide TFTs on a 300-nm-thick SiO_2 gate dielectric layer thermally grown on a doped p-type Si wafer. The silicon substrates were cleaned with deionized water, isopropyl alcohol and acetone ultrasonically. Substrates were then treated with UV radiator for 10 min to remove organics and to improve adhesion. The precursor solution for fabricating ZTO was prepared by dissolving 0.30-M zinc acetate dihydrate ($Zn(CH_3COO)_2{\cdot}2H_2O$) and 0.30-M tin chloride ($SnCl_2$) in a mixed solution of 20 ml of 2-metoxyethanol and 0.6 ml of actylacetone. After the solute and solvent had been mixed the mixture was stirred for 8 h at room temperature. Thiourea (NH_2CSNH_2) with different mole percentages of 0.30 M, 0.24 M, 0.18 M, 0.12 M and 0.06 M was added to the ZTO solution. After the solution had been stirred for 20 min at 120 °C, it was stirred for 3 h more at room temperature and was then aged for 24 h. The prepared solution was filtered through a 0.2-μm polytetrafluoroethylene (PTFE) syringe filter and spin-coated at 5000 rpm for 50 s. A prebake was carried out at 100 °C for 1.5 minutes on a hotplate and the sample was annealed at 600 °C for 1 h in a furnace. Al source/drain electrodes 100-nm thick, were thermally evaporated with a shadow mask. The channel width and length were 1500 μm and 100 μm, respectively. The transfer characteristics of fabricated TFTs were measured by using a computer-interfaced DC voltage source and picoammeter. The hysteresis characteristics were measured using a gate-voltage sweep from −15 V to 15 V with a drain voltage of 5 V. The light stability was measured for up to 2,400 sec under illumination with white light from a halogen lamp.

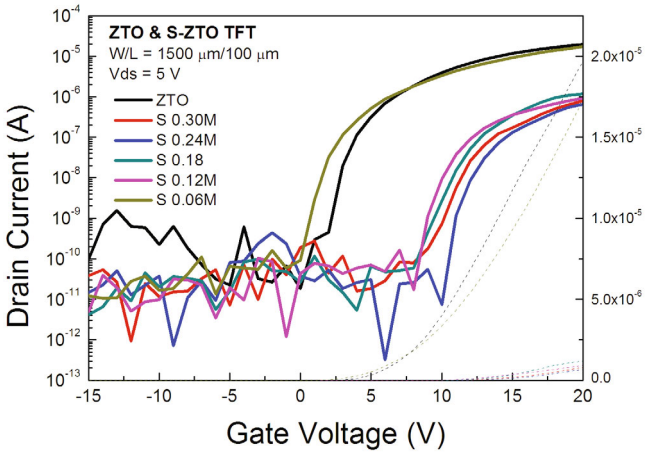

Fig. 1. (Color online) Transfer characteristics of the S-ZTO TFTs at various concentrations.

III. RESULTS AND DISCUSSION

In order to investigate the effect of sulfur on the device properties of the solution-processed S-ZTO TFTs, we measured the transfer characteristics for the TFTs fabricated with different sulfur concentrations. Figure 1 shows the transfer curves of fabricated S-ZTO TFTs as a function of the sulfur concentration. With increasing of sulfur concentration, the threshold voltage increased whereas the on-current and the mobility decreased. The decrease in the mobility with increasing sulfur concentration was attributed to the scattering that occurred due to the incorporated sulfur atoms, which have a larger size than the oxygen atoms. The electrical properties of the fabricated S-ZTO TFTs are summarized in Table 1. As listed in Table 1, the best device characteristics, which include a threshold voltage of −0.74 V, a sub-threshold swing of 0.67 V/dec, on/off current ratio of of 8.31×10^5, and a mobility of 0.70 cm^2/Vs, were observed for 0.06-M S-ZTO TFTs. The S-ZTO TFT with 0.06 M sulfur shows the better electrical properties then the other S-ZTO TFTs with sulfur concentrations larger than 0.06 M. We also emphasize here that the device properties of 0.06-M S-ZTO TFTs were similar to those of ZTO TFTs without S.

Figures 2(a) and (b) show the transfer characteristics of ZTO and 0.06-M S-ZTO TFTs, respectively, which were measured under dark and illuminated conditions. As the time of light illumination increased, a negative threshold voltage shift was observed, and the off-current was increased, which was attributed to increase a number of in free electrons due to the ionization of oxygen vacancies. The conductivity of oxide semiconductors has been reported to be increased when they are exposed to light, especially with wavelengths shorter than 450 nm. Ionized oxygen vacancy(Vo^{2+}), as well as other elements such as hydrogen and zinc interstitials, are well known to play a key role as a donor and generator of free elec-

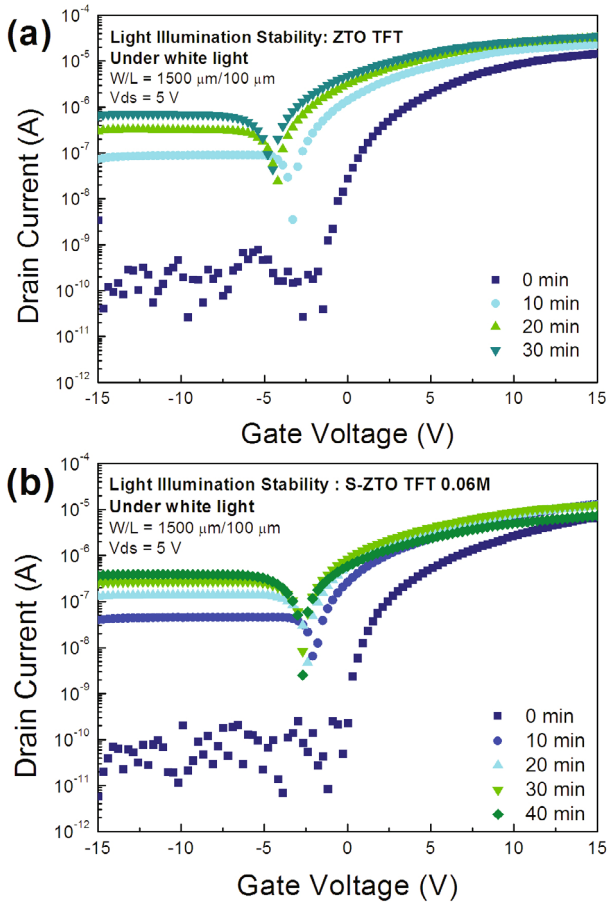

Fig. 2. (Color online) (a) Transfer characteristic of ZTO TFT after light illumination, (b) Transfer characteristic of S-ZTO TFT after light illumination.

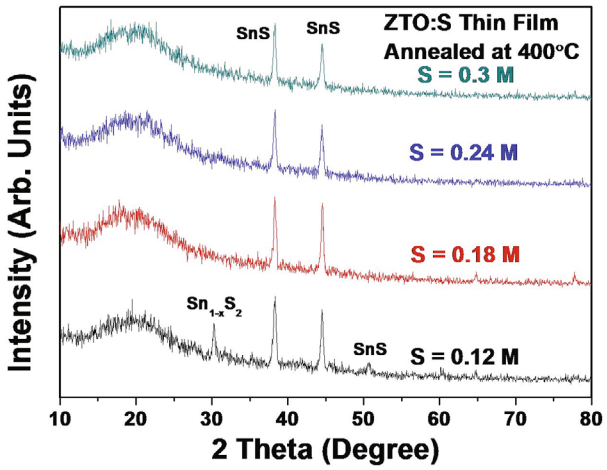

Fig. 3. (Color online) XRD data for S-ZTO thin film with different sulfur concentrations.

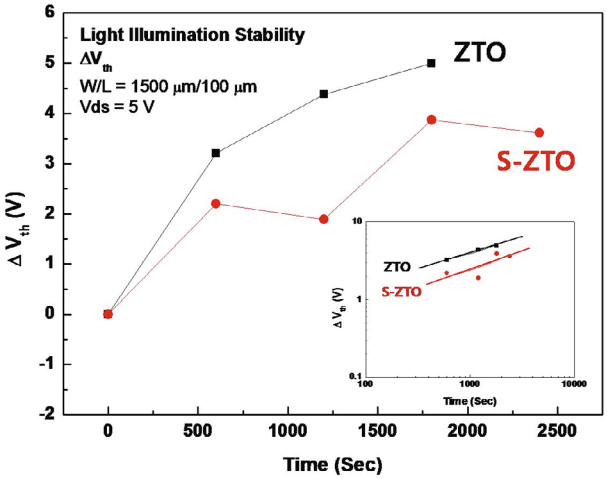

Fig. 4. (Color online) ΔV_{th} of ZTO and S-ZTO TFT as a function of the illumination time.

trons in the conduction band. Therefore, we conclude that the increasing the off-current with light illumination, as shown in Fig. 2, is attributed to the increase in the number of Vo^{2+} due to light illumination. Figures 2(a) and (b) show that off-currents for the S-ZTO TFTs are lower than those for the ZTO TFTs, which is related to a reduction in the number of oxygen vacancies carried by sulfur incorporation. The lower number of oxygen vacancies carreid by sulfur incorporation results in a lower concentration of Vo^{2+} in S-ZTO TFTs than in the ZTO TFT.

Figure 3 shows XRD data for S-ZTO thin films with different sulfur concentrations, indicating that the incorporated sulfur atoms from covalent bonds with tin atoms, which reveals that the sulfur atoms reduce the density of oxygen vacancies, resulting in less dark off-conductivity after light illumination for S-ZTO TFT.

As shown in Fig. 4, the threshold voltage shifts more negatively, and the increment of the threshold voltage, ΔV_{th}, increases with increasing time of light illumination. We also observed that the ΔV_{th} of the ZTO TFT was 5 V while that of the 0.06-M S-ZTO TFT was less than 4 V after 1800 seconds of illumination. This suggests that under the light irradiatetion, the ΔV_{th} of the 0.06-M S-ZTO TFT was less than that of ZTO TFT. With the off-conductivity results after illumination, the lower number of oxygen vacancies in the S-ZTO gave less threshold voltage variation due to lower number of oxygen vacancies being lower than that of ZTO because a lower number of oxygen vacancies results in fewer ionized oxygen vacancies of the donor.

The hysteresis in the transfer curve is shown in Figs. 5(a) and (b) for ZTO and S-ZTO, respectively. Hysteresis for the 0.06-M S-ZTO TFT is less than that for the ZTO TFT. As observed with other passivation effects of sulfur on the gate dielectric interface [31–33], the replacement of oxygen by sulfur reduces the number of interface defects related to the oxygen. The reduced number of trap states carried by the sulfur reduces the hysteresis for S-ZTO. The hysteresis is attributed to charge trapping during the measurement, which becomes larger with increasing number of trap states.

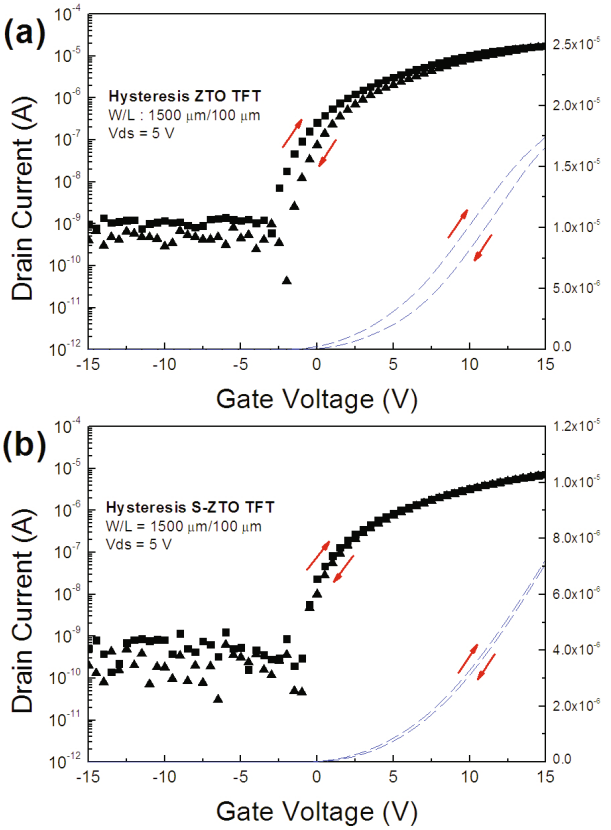

Fig. 5. (Color online) (a) Hysteresis characteristics of ZTO TFT, (b) Hysteresis characteristics of S-ZTO TFT.

IV. CONCLUSION

We investigated the effect of sulfur incorporation on the electrical properties and the stability characteristics of ZTO TFTs. The higher mobility of the ZTO TFTs with less S incorporation is related to the smaller concentration of sulfur. We observed that the device properties of 0.06-M S-ZTO TFTs were similar to those of ZTO TFTs without added S. We also found that the lower off-current for the S-ZTO TFTs compared to that for the ZTO TFTs was related to the reduced number of oxygen vacancies carried by sulfur incorporation. The XRD analysis confirmed that the filling of oxygen sites by sulfur atoms reduces the density of the oxygen vacancies and results in less dark off-conductivity for S-ZTO TFTs compared to ZTO TFTs after light illumination. Therefore, based on the experimental results, we conclude that the improved stabilities observed in S-ZTO TFTs are attributed to the number of oxygen vacancies.

REFERENCES

[1] A. J. Snell, K. D. Mackenzie, W. E. Spear, P. G. LeComber and A. J. Hughes, Appl. Phys. **24**, 357 (1981).
[2] A. Nathan, G. R. Chaji and S. J. Ashtiani, Display Tech **1**, 267 (2005).
[3] S. Uchikoga and N. Ibaraki, Thin Solid Films **383**, 19 (2001).
[4] J. H. Lee, W. J. Nam, B. K. Kim, H. S. Choi, Y. M. Ha and M. K. Han, IEEE Trans. Device Lett. **27**, 830 (2006).
[5] T. Kamiya, K. Nomura and Hideo Hosono, Sci. Technol. Adv. Mater. **11**, 044305 (2010).
[6] M. Kimura, T. Nakanishi, K. Nomura, T. Kamiya and H. Hosono, Appl. Phys. Lett. **92**, 133512 (2008).
[7] J. G. Um, M. Mativenga and J. Jang, Appl. Phys. Lett. **103**, 033501 (2013).
[8] K. M. Yu, H. J. Moon, M. K. Ryu, K. I. Cho, E. J. Yun and B. S. Bae Jpn. J. Appl. Phys. **51**, 09MF11 (2011).
[9] M. Mativenga, J. W. Choi, J. J. Hur, H. J. Kin and J. Jang, J. Info. Disp. **12**, 47 (2011).
[10] K. M. Yu, J. T. Yuh, S. H. Ko Park, M. K. Moon, M. K. Ryu, E. J. Yun and B. S. Bae, Jpn. J. Appl. Phys. **52**, 10MA12 (2013).
[11] E. Fortunato, N. Correia, P. Barquinha, L. Pereira, G. Goncalves and R. Martins, IEEE Electron Device Lett. **29**, 988 (2008).
[12] P. Barquinha, L. Pereira, G. Goncalves, R. Martins and E. Fortunato, Electron chem. Solid-State Lett. **11**, H248 (2008).
[13] K. Nomura, H. Ohta, K. Ueda, T. Kamiya, M. Hirano and H. Hosono, Science **300**, 1269 (2003).
[14] J. F. Wager, Science **300**, 1245 (2003).
[15] H. S. Bae, M. H. Yoon, J. H. Kim and S. Im, Appl. Phys. Lett. **83**, 5313 (2003).
[16] A. Tsukazaki, A. Ohtomo, T. Kita, Y. Ohno, H. Ohno and M. Kawasaki, Science **315**, 1388 (2007).
[17] A. P. Ramirez, Science **315**, 1377 (2007).
[18] B. N. Pal, J. Sun, B. J. Jung, E. Choi, A. G. Andreou and H. E. Katz, Adv. Mater. **20**, 1023 (2008).
[19] S. H. Ko, I. Park, H. Pan, N. Misra, M. S. Roger, C. P. Grigoropoulos and A. P. Pisano, Appl. Phys. Lett. **92**, 154102 (2008).
[20] S. J. Heo, D. H. Yoon, T. S. Jung and H. J. Kim. J. Info. Disp. **14**, 79 (2013).
[21] G. H. Kim, H. S. Shin, B. D. Ahn, K. H. Kim, W. J. Prak and H. J. Kim, Eleccro chem. Soc. **156**, H7 (2004).
[22] E. Bacaksiz, M. Parlak, M. Tomakin, A. Ozcelik, M. Karakiz and M. Altungbas, J. Alloys Compd. **466**, 447 (2008).
[23] S. J. Seo, C. G. Choi, Y. H. Hwang and B. S. Bae, J. Phys. D: Appl. Phys. **42**, 035106 (2009).
[24] W. H. Jeong, G. H. Kim, D. L. Kim, H. S. Shin, H. J. Kim, M. K. Ryu, K. B. Park, J. B. Seon and S. Y. Lee, Thin Solid Films **519**, 5740 (2011).
[25] Y. H. Jung, W. S. Yang, C. Y. Koo, K. K. Song and J. H Moon, J. Mater. Chem. **22**, 5390 (2012).
[26] J. C. Do, C. H. Ahn, H. K. Cho and H. S. Lee, J. Phys. D: Appl. Phys. **45**, 225103 (2012).
[27] J. S. Seo, J. H. Jeon, Y. H. Hwang, H. J. Park. M. K. Ryu, S. H. Ko Park and B. S. Bae, Sci. Rep. **3**, 2085 (2013).
[28] R. Zhang, B. Wang, H. Zhang and L. Wei, Appl. Surf. Sci. **241**, 435 (2005).
[29] Y-Z. Yoo, Z-W. Jin, T. Chikyow, T. Fukumura, M. Kawasaki and H. Koinuma, Appl. Phys. Lett. **81**, 3798 (2002).

[30] S. Y. Jeon, S. H. Bang, S. J. Lee, S. Y. Kwon, W. H. Jeong, H. J. Chang, H. H. Park and H. T. Jeon, J. Korean Phys. Soc. **53**, 3287 (2008).
[31] D. Y. Petrovykh, M. J. Yang and L. J. Whitman, Surf. Sci. **523**, 231 (2003).
[32] J. D. Hwang, D. S. Lin, Y. L. Lin, W. T. Chang and C. H. Yang, Thin Solid Films **519**, 833 (2010).
[33] K. Dileep and R. Datta, Alloys Com. **586**, 499 (2014).